

perature of the heat bath controlling the cooling. This process is illustrated schematically in Fig. 1.

Let the actual (as opposed to the measured) entropy of the glass be S_g . The initial entropy of the entire system is $S_l(T_M) + S_{\text{bath}}(T_M)$. Since the glass is not in equilibrium, it does not have a well-defined temperature, and we cannot compute the change in S_g calorimetrically. On the other hand, the bath *is* in equilibrium, and its entropy changes by $\int(\dot{Q}/T)dt$. Now the heat bath and glass together comprise a closed system, and the entropy of a closed system must increase with time. Hence,

$$S_l(T_M) + S_{\text{bath}}(T_M) \leq S_g(T_1) + S_{\text{bath}}(T_M) - \int_{T=T_M}^{T=T_1} (\dot{Q}/T) dt,$$

or

$$S_g(T_1) \geq S_{\text{cool}}(T_1). \tag{3}$$

The measurement of the entropy on cooling therefore yields a lower bound on the actual (statistical) entropy of the glass.

To measure the entropy on heating, S_{heat} , one would take the glass at the low temperature T_1 , and measure

how much heat has to be added to reach the liquid state,

$$S_{\text{heat}}(T_1) + \int_{T=T_1}^{T=T_M} (\dot{Q}/T) dt = S_l(T_M).$$

Again, the measured quantity is the change in entropy of the heat bath, $-\int_{T=T_1}^{T=T_M} (\dot{Q}/T) dt$. Since the total entropy of the glass plus heat bath system must increase,

$$S_g(T_1) \leq S_l(T_M) - \int_{T=T_1}^{T=T_M} (\dot{Q}/T) dt,$$

we find that

$$S_{\text{cool}}(T_1) \leq S_g(T_1) \leq S_{\text{heat}}(T_1). \tag{4}$$

The measurement of the entropy on heating therefore yields an upper bound on the actual entropy. Notice that we have not said exactly what is meant by the ‘‘entropy’’ of the glass, S_g . That is, we have not specified how one is to take the trace in (2).⁴ It is clear, however, that any reasonable definition of the glassy entropy must satisfy the bounds (4).

Our first example, Fig. 2, shows the thermodynamic entropies measured while heating and cooling a model orientational glass in a Monte Carlo simulation.⁵ The error bars shown represent the error in the *mean* of the data; fifty runs were necessary to establish the bounds for the fastest cooling rate and five for the slowest. Two runs of the simulation, cooled in the same manner, have different thermodynamic entropies because internal relaxations take place at different times.⁶ The means of the probability distributions $\rho(S)$ of thermodynamic entropies on heating and cooling give the bounds on the statistical entropy. Furthermore, the entire distribution is an intrinsic property of the glass and its thermal history.

As the second example, consider the simplest possible model of a glass, a single two-level system (TLS). A TLS is always in one of two possible states, or ‘‘wells,’’ whose energies differ by an asymmetry ϵ . Transitions

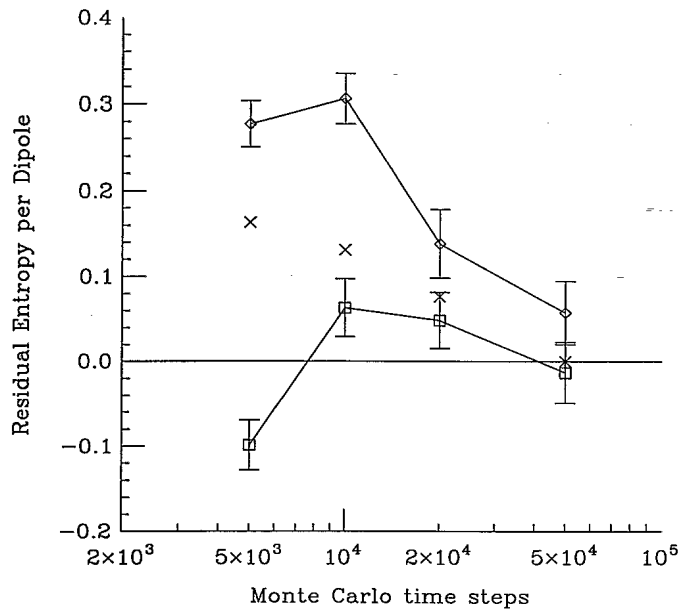


FIG. 2. Residual entropy as a function of cooling time. $T=0$ statistical entropy (crosses) and upper and lower entropy limits (diamonds and squares) from a Monte Carlo simulation (Ref. 5) of a model orientational glass of elastic dipoles. The system contained sixteen dipoles, and was cooled and heated between 1000 and 0 K. The error bars on the upper and lower limits were all about 0.03. The errors on the statistical entropy were not computed. The computer time needed to get the statistical entropy grows exponentially with the system size. We can compute the statistical entropy in this case only because the system is small. All material properties of glasses depend on the cooling rate, including the residual entropy.

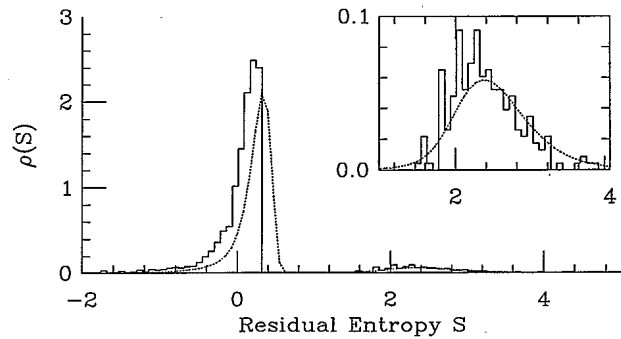


FIG. 3. The solid line is the distribution at $T=0$ of the ‘‘thermodynamic’’ entropy $\int dQ/T$ measured in a Monte Carlo simulation of a single two-level system. The dotted line is the asymptotic expression for the same distribution. Inset: The upper peak represents occasions on which the system was trapped in the upper well.

between the states take place by thermal activation over a free-energy barrier of height V with attempt frequency Γ_0 . Since the transition rate is highly temperature dependent,⁷ if the system is cooled at a finite, nonzero rate the TLS will "freeze" into a nonequilibrium configuration at a temperature T^* when the transition rate becomes slower than the cooling rate. Figure 3 shows the distribution of S_{cool} for a TLS at zero temperature, with⁸ $T(t) = T_0/(1 + Rt)$. The significant features of the distribution are the two peaks and the long tail on the lower peak.

The upper peak in the distribution represents coolings in which the system was left in the upper well. If the probability of finding the system in the upper well and simultaneously finding the measured thermodynamic entropy to be between S and $S + dS$ is $\rho_1(S)dS$, and the corresponding probability of finding the system in the lower well is $\rho_l(S)dS$, then near equilibrium $\rho_1(S)$ must be peaked around the value $\langle S_1 \rangle_{\text{eq}} = -\ln n$, and $\rho_l(S)$ must be peaked around $\langle S_l \rangle_{\text{eq}} = -\ln(1 - n)$, where n is the total probability of being in the upper well. Since the total distribution $\rho(S) = \rho_l(S) + \rho_1(S)$, and transitions between the two states transfer energy ϵ to and from the surrounding heat bath, the peaks in $\rho(S)$ must be separated by $\beta\epsilon$. As the temperature falls and transitions take place with larger $\beta\epsilon$, the peaks move apart. Below T^* transitions between the wells are not frequent enough to maintain the ever increasing equilibrium peak spacing. At zero temperature the separation is determined by T^* , not T .

The long tail in the entropy distribution results from transitions that take place after the TLS falls out of equilibrium. At T^* the two peaks are separated by $\beta^*\epsilon$. Each subsequent downward transition removes weight from the high S peak, and moves it by $\beta\epsilon > \beta^*\epsilon$ down the entropy scale to the low entropy side of the lower peak, forming the tail. The rate of downward transitions is small, but in this regime the rate of upward transitions is infinitesimal, so the low-entropy tail is not diminished by transitions back to the upper well.

Real glasses are always cooled much more slowly than computer simulations. Therefore, it will be important to understand the entropy distribution of a TLS cooled asymptotically slowly. Following Huse and Fisher,⁹ who discussed the zero-temperature residual energy of a TLS, we define a dimensionless asymmetry $\mu = \epsilon/V$ and a dimensionless cooling rate $\delta = RV/\Gamma_0 T_0$. Since δ is roughly the rate of the microscopic oscillation time to the macroscopic cooling time, we expect physical systems to have $\delta \ll 10^{-12}$. Figure 3 shows the zero-temperature entropy distribution for a TLS with $\epsilon/V = 0.5$ and $\delta = 0.01$. The solid line is the result of a Monte Carlo simulation, while the dotted line is the prediction of the asymptotic analysis.¹⁰ Letting $\tilde{\rho}(\sigma)$ be the Fourier transform of $\rho(S)$, and defining a convenient temperature variable $x \equiv \exp(-\beta V)$, for asymptotically small δ we find

$$\frac{\tilde{\rho}_1(\sigma, x)}{\tilde{\rho}_l(\sigma, x)} = \frac{\exp(-x/\delta)}{\delta^{\mu(1-i\sigma)} \Gamma[1 + \mu(1-i\sigma), x/\delta]}, \quad (5)$$

and

$$\ln \tilde{\rho}_1(\sigma, x) \tilde{\rho}_l(\sigma, x) = f(\sigma) + \frac{1}{\delta} \int_x^1 dz \left[1 + z^\mu + z^{\mu(1-i\sigma)} \frac{\tilde{\rho}_l(\sigma, z)}{\tilde{\rho}_1(\sigma, z)} - z^{i\sigma\mu} \frac{\tilde{\rho}_1(\sigma, z)}{\tilde{\rho}_l(\sigma, z)} \right]. \quad (6)$$

Here Γ is the incomplete Γ function, and $f(\sigma)$ depends on the initial high-temperature distribution. Considering that $\delta = 0.01$ is not very small, the agreement between the curves in Fig. 3 is remarkable. For physical cooling rates, the agreement should be excellent.

The entropy distribution is useful as a tool for examining the dynamics of complicated nonequilibrium systems. As the third example, we use the distribution to examine a small (5×5) two-dimensional $\pm J$ Ising spin-glass.¹¹ Figure 4 shows the entropy distribution obtained by cooling the spin-glass repeatedly from $T = 10J$ to $T = 0$ in 1000 Monte Carlo steps. The two peaks and the long low entropy tail show that this particular spin-glass looks like a TLS at low temperatures. The separation of the two maxima in the distribution shows that $\beta^*\epsilon = 0.17$. We can also determine β^* and ϵ separately, by varying the cooling schedule. Figure 4 also shows the entropy distribution derived by cooling the spin-glass at a constant rate of 100 Monte Carlo steps per degree from high temperature to a temperature $T_1 < T^*$. The glass was then instantaneously quenched to $T_2 < T_1$, at which point the cooling was resumed at the previous rate. No

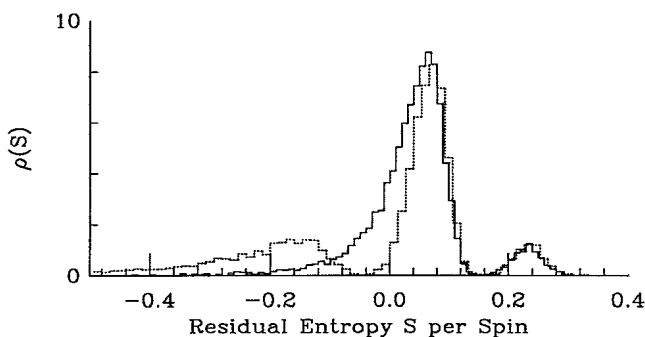


FIG. 4. The solid line is the distribution of entropies measured by cooling a 5×5 Ising spin-glass 10000 times from $T = 10J$ to $T = 0$ Monte Carlo steps. The average thermodynamic entropy is 0.033 per spin; the statistical entropy (determined by our counting zero-temperature states) is 0.072 per spin, and the average entropy measured on heating (not shown) is 0.095 per spin, so the thermodynamic entropy does indeed bound the statistical entropy. The dotted line is the distribution for the same system, but quenched from $T = 0.7J$ to $T = 0.4J$. The hole in the distribution is determined by the effective TLS asymmetry ϵ and the freezing temperature T^* .

transitions from the upper state occurred, therefore, between T_1 and T_2 , so there is no weight in the entropy tail between $\langle S_{\uparrow} \rangle_{\text{eq}} - \beta_2 \epsilon$ and $\langle S_{\uparrow} \rangle_{\text{eq}} - \beta_1 \epsilon$. The hole is of width $(\beta_2 - \beta_1) \epsilon$, which determines ϵ , and hence β^* . For the example in Fig. 4, $T_1 = 0.7J$, $T_2 = 0.4J$, the hole in the distribution is of width ≈ 0.1 , implying that $\epsilon \approx 0.09$, and that $T^* \approx 0.5J$. Because this system is small, we have actually found the states of the spin-glass corresponding to the wells of the TLS, and have confirmed that the measurements of ϵ and T^* are correct. Notice that, even if the upper peak in the distribution were completely absent at $T=0$, we could still determine ϵ by this method, although we would have to go to greater lengths to find β^* .

Two problems (at least) chronically plague computer simulations of glasses: large fluctuations due to the finite size of the system, and the difficulty of reaching equilibrium. The entropy distribution is an easily measurable quantity that makes an asset of both of these difficulties. Furthermore, it depends on the entire history of the glass, and at least in a simple model is analytically calculable in the limit of slow cooling rates.

The authors would like to thank Richard Palmer, Paul Sulewski, and Eric Grannan for their assistance. We would especially like to thank Alan Dorsey for help with the asymptotic analysis. This work was supported by National Science Foundation Grant No. DMR-8451921, and conducted with use of the Cornell National Supercomputer Facility, funded in part by the National Science Foundation, New York State, and IBM.

¹For a summary of some zero-temperature entropy measurements see G. P. Johari, *Philos. Mag. B* **41**, 41 (1980). One of the earliest measurements was by G. E. Gibson and W. F. Giauque, *J. Am. Chem. Soc.* **45**, 93 (1923).

²We estimate the bounds to be separated by roughly 1% in a real glass cooled at a practical rate.

³R. Ettelaie and M. A. Moore, *J. Phys. (Paris) Lett.* **46**, L893 (1985), computed the residual entropy S_{cool} of a one-dimensional spin-glass simulation, to test whether it is related to the density of states N measured at the residual energy. They found in this system that $S_{\text{cool}} \leq \ln N$, and approaches it at slow cooling rates. Here we show that $S_{\text{cool}} \leq S_g$, the statistical entropy. In retrospect their results are consistent with $S_g = \ln N$ (which we have no reason to believe will be true in general).

⁴R. Palmer, *Adv. Phys.* **31**, 669 (1982).

⁵E. R. Grannan, M. Randeria, and J. P. Sethna, *Phys. Rev. Lett.* **60**, 1402 (1988). Further details to be published.

⁶On any given run, the entropy measured on heating is not even necessarily above that measured on cooling.

⁷Transitions from the upper well to the lower take place at a rate Γ_{\downarrow} , and transitions from the lower well to the upper take place at a rate $\Gamma_{\uparrow} = e^{-\beta\epsilon} \Gamma_{\downarrow}$, where $\beta \equiv 1/T$. In the absence of quantum mechanical tunneling between the wells, $\Gamma_{\uparrow\downarrow} = \Gamma_{\downarrow} e^{-\beta V}$. The population n of the upper well is found from the master equation $\dot{n} = \Gamma_{\uparrow}(T)(1 + e^{-\beta\epsilon})[n_0(T) - n]$, where $n_0(T) = e^{-\beta\epsilon}/(1 + e^{-\beta\epsilon})$ is the equilibrium value of n .

⁸In the first and third simulations, we cool linearly to zero temperature, $T(t) = T_0 - \dot{T}t$. The asymptotics in the second simulation is simplified with use of the more gradual cooling rate $T(t) = T_0/(1 + Rt)$.

⁹D. A. Huse and D. S. Fisher, *Phys. Rev. Lett.* **57**, 2203 (1986).

¹⁰A. Dorsey, S. A. Langer, and J. P. Sethna, to be published. This paper will include versions of Eqs. (5) and (6) uniformly valid in μ .

¹¹This model was chosen for its simplicity and computational speed. The spins sit on a square lattice with periodic boundary conditions. The Hamiltonian is $H = -\sum_{\langle ij \rangle} J_{ij} S_i S_j$, where the spins $S_i = \pm 1$ and the bonds J_{ij} are chosen at random to be either ferromagnetic ($J_{ij} = 1$) or antiferromagnetic ($J_{ij} = -1$). The entropy was set to be $\ln 2$ per spin at high temperature. Naturally, larger simulations will exhibit much more complicated phenomena.